T-lean fuel assemblies for MHD direct conversion

Develop and benchmark MCAD model based on Tabak's Case C run[1] for isobaric hot spot ignition (see Fig. 1) with his f = 0.1 tritium parameter (to maximize non-neutron yield for direct conversion with ηG_f>100 for low recirculating power)

TABAK

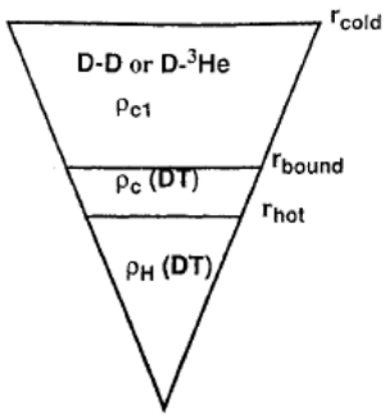

FIG. 1. Pie diagram of compressed core.

[1] Max Tabak, Nuc. Fusion 36, No2 (1996). Calculates DD burn assuming 10 keV initial DT hot spot. (If needed, a late shock (Betti- Perkins) could be applied to insure ignition at lower implosion velocities and at lower adiabats, say α=1.5 instead of at α=2 as Max assumed). We assume DD main fuel instead of D-^{3}He for reasons Max stated.

Fuel assembly energy (variable) (MJ) $\quad ORIGIN := 1$

Min tritium loading parameter for ηG>100

For $i := 1..7$ $\quad Ef_i := 0.05 + 0.05 \cdot i^2$ fuel energy cases

$f := 0.1$ $\quad r_{bound}(r_{hot}) := r_{hot} \cdot (1 + 2 \cdot f)$ DT radius

$\zeta := 1 - (1 + 2 \cdot f)^{-3}$ DT load parameter

Use Max's formulary[1] for fuel assemblies optimizing gain for given fuel energies:

Cold DD fuel density in g/cm3) $\quad \rho_{cdd}(\alpha, E_f) := 0.8 \cdot 1050 \cdot \left(\alpha^2 \cdot E_f\right)^{-0.3}$ Eq 1

Hot spot fuel density (g/cm3) $\quad \rho_{hdt}(E_f) := 63 \cdot E_f^{-0.5}$ Eq 2

Hot spot radius (cm) $\quad r_{hdt}(E_f) := 0.0063 \cdot E_f^{0.5}$ Eq 3

Radius of pure DT region (Case C) $\quad r_{bdt}(E_f) := (1 + 2 \cdot f) \cdot r_{hdt}(E_f)$ Eq 4

Outer DD fuel radius (Tabak) (cm) $\quad r_{cdd}(E_f) := \left[\left[\left(3 \cdot r_{hdt}(E_f)\right)^3 - r_{bdt}(E_f)^3\right] \cdot 1.25 + r_{bdt}(E_f)^3\right]^{0.333}$ Eq 5

Mass of cold D fuel (g) $\quad M_d(\alpha, E_f) := 4 \cdot 3^{-1} \cdot \pi \cdot \left(r_{cdd}(E_f)^3 - r_{hdt}(E_f)^3\right) \cdot \rho_{cdd}(\alpha, E_f)$ Eq 6

Mass of DT hot spot (g) $\quad M_{hdt}(E_f) := 4 \cdot 3^{-1} \cdot \pi \cdot r_{hdt}(E_f)^3 \cdot \rho_{hdt}(E_f)$

Total initial T fuel mass (g) (Case C) $\quad M_t(\alpha, E_f) := 0.6 \cdot \left(M_{hdt}(E_f) + \frac{\zeta}{0.8} \cdot \frac{4}{3} \cdot \pi \cdot r_{bdt}(E_f)^3 \cdot \rho_{cdd}(\alpha, E_f)\right)$ Eq 7

Rho-r of total fuel assembly (g/cm^2) $\quad \rho r(\alpha, E_f) := \rho_{hdt}(E_f) \cdot r_{hdt}(E_f) \ldots$ Eq 8

$+ 1.25 \cdot \rho_{cdd}(\alpha, E_f) \cdot \left(r_{bdt}(E_f) - r_{hdt}(E_f)\right) \ldots$

$+ \rho_{cdd}(\alpha, E_f) \cdot \left(r_{cdd}(E_f) - r_{bdt}(E_f)\right)$

Burnup fractions (Fig.2) ~ ρr / ($\rho r + H_B$) depend on T which increases with ρr:

f	Main fuel composition	Column density (g/cm^2)	Peak hotspot temperature (keV)	Main fuel temperature (keV)
0.033	D	4.6	40	4
0.033	D	12	100	8
0.166	D	4.6	90	16
0.166	D	12	210	50
0.033	0.01 T/0.5 D	4.6	70	13
0.033	0.01 T/0.5 D	12	210	80
0.033	0.04 T/0.5 D	4.6	180	160
0.033	0.04 T/0.5 D	12	310	160

(From Tabak- Table 1)

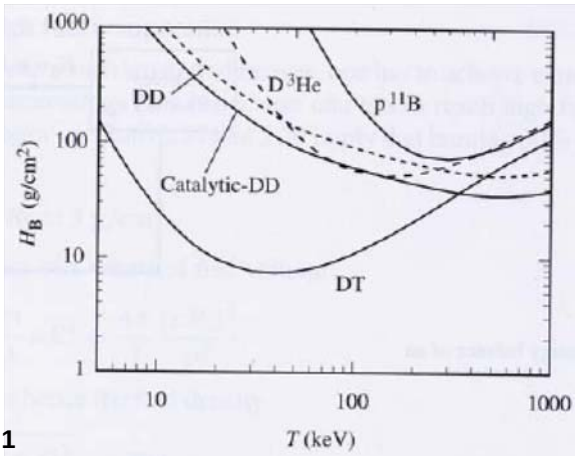

 Figure 1

Model for burnup fractions. Note in Table 1 as ρr increases from 4.6 to 12 g/cm2 (factor of 2.6), temperatures for DT hotspot and DD main fuel increase by a similar factors. Fig. 2 shows those temperature changes raise H_B for DT ~ 2 times, while decreasing H_B for DD by ~3 times. We use this to fit the coefficients for the model H_B terms in Fig. 9 and 10 below.

Est burnup fraction of DD (constant fitted to Tabak's Case C runs).

$$f_{bd}(\alpha, E_f) := \rho r(\alpha, E_f)\cdot\left(\rho r(\alpha, E_f) + 1600\cdot\rho r(\alpha, E_f)^{-1.2}\right)^{-1} \qquad \text{Eq 9}$$

Est burnup fraction of initial DT load

$$f_{bt}(\alpha, E_f) := \rho r(\alpha, E_f)\cdot\left(\rho r(\alpha, E_f) + 2\cdot\rho r(\alpha, E_f)^{0.8}\right)^{-1} \qquad \text{Eq 10}$$

D(d,p)T and D(d,n)3He branching @ 100 keV relative energy $\quad f_p := 0.48 \quad f_n := 0.52$

Est. yield (MJ) = initial T burnup @ f_{bt}

+ D-D burnup yield @ f_{bd}

+ bred T burnup yield @ f_{bt}

+bred 3He burnup yield assuming $fb_{3He} \sim f_{bd}$.

$$Y_f(\alpha, E_f) := 5\cdot 3^{-1}\cdot M_t(\alpha, E_f)\cdot f_{bt}(\alpha, E_f)\cdot\left(3.37\cdot 10^5\right) \ldots + M_d(\alpha, E_f)\cdot f_{bd}(\alpha, E_f)\cdot\left(\begin{array}{l} 8.85\cdot 10^4 \ldots \\ + 1.25\cdot f_p\cdot f_{bt}(\alpha, E_f)\cdot 3.37\cdot 10^5 \ldots \\ + 1.25\cdot f_n\cdot f_{bd}(\alpha, E_f)\cdot 3.5\cdot 10^5 \end{array}\right) \qquad \text{Eq 11}$$

Table 2: Fuel assembly parameters for Max Tabak's Case C for T-lean fuel assemblies with T localized near hotspot, DD main fuel, with f = 0.1 T-load parameter, and adiabat α=2

$i =$	Fuel energy $Ef_i =$	Deuterium density $\rho_{cdd}(2, Ef_i)$	Hot spot DT radius $\frac{r_{hdt}(Ef_i)}{=10^{-4}}$	Outer-D radius $\frac{r_{cdd}(Ef_i)}{10^{-4}}$	D-Mass load $\frac{M_d(2, Ef_i)}{10^{-3}}$	T-Mass load $\frac{M_t(2, Ef_i)}{10^{-3}}$	Rho-r total $=\rho r(2, Ef_i)$	D-burn fraction $f_{bd}(2, Ef_i)$	T-burn fraction $f_{bt}(2, Ef_i)$	Fusion yield $Y_f(2, Ef_i) =$
1	0.1	1106	20	64	1.2	0.02	5.4	0.025	0.412	11
2	0.25	840	32	102	3.6	0.07	6.4	0.036	0.42	40
3	0.5	682	45	144	8.3	0.16	7.3	0.048	0.427	111
4	0.85	582	58	188	15.6	0.29	8.1	0.059	0.432	245
5	1.3	512	72	232	26	0.49	8.8	0.069	0.436	466
6	1.85	461	86	277	39.7	0.74	9.4	0.08	0.439	798
7	2.5	421	100	322	56.9	1.05	10	0.089	0.442	1268
	(MJ)	(g/cm^3)	(μm)	(μm)	(mg)	(mg)	(g/cm^2)			(MJ)

Note in Table 2 that these cases correspond to inital tritium molar fractions of only 1.3 percent for the whole fuel assembly. Less than half the initial and bred tritium burns up despite the large column densities ρr~ 10 because the burn temperature much exceeds the 40 keV optimum for burnup.

Internal (fuel) energy gains

M.Tabak results[1] for fuel gain G_{mt} for his Case C: $Gmt_1 := 105$ $Gmt_2 := 160$ $Gmt_3 := 230$ $Gmt_4 := 295$ $Gmt_5 := 360$ $Gmt_6 := 430$ $Gmt_7 := 500$

$$G_f(\alpha, E_f) := Y_f(\alpha, E_f) \cdot E_f^{-1} \qquad \text{Eq 12}$$

$i =$	$Ef_i =$	$G_f(2, Ef_i) =$
1	0.1	109
2	0.25	161
3	0.5	222
4	0.85	288
5	1.3	358
6	1.85	431
7	2.5	507

Fig. 2: Fuel gain G_f (model) and in Tabak's Case C vs. fuel energy E_f

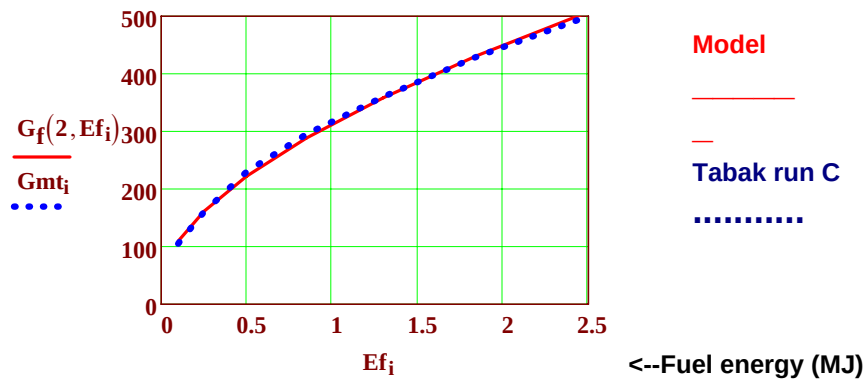

Fig 2 shows the model and the Case C runs agree well. (good enuf for government work).

Next lets consider T-breeding:

Mass of T-bred in-situ by D+D-->T+p branch (g) $$M_{tb}(\alpha, E_f) := 0.75 \cdot f_p \cdot M_d(\alpha, E_f) \cdot f_{bd}(\alpha, E_f) \qquad \text{Eq 13}$$

Mass of 3He-bred by D+D-->3He+n branch (g) $$M_{3Heb}(\alpha, E_f) := 0.75 \cdot f_n \cdot M_d(\alpha, E_f) \cdot f_{bd}(\alpha, E_f) \qquad \text{Eq 14}$$

Total T consumed by fusion (g) $$M_{tc}(\alpha, E_f) := \left(M_t(\alpha, E_f) + M_{tb}(\alpha, E_f)\right) \cdot f_{bt}(\alpha, E_f) \qquad \text{Eq 15}$$

Net T mass gain (loss) (g) $$M_{tn}(\alpha, E_f) := M_{tb}(\alpha, E_f) - M_{tc}(\alpha, E_f) \qquad \text{Eq 16}$$

In-situ Neutrons per Triton burned $$N_{ndd}(\alpha, E_f) := \left(M_{3Heb}(\alpha, E_f) + M_{tc}(\alpha, E_f)\right) \cdot M_{tc}(\alpha, E_f)^{-1} \qquad \text{Eq 17}$$

Note by inspection, if all tritium were burned up, and the DD breeding of T dominated over the initial T load, the maximum N_{nt} max =2. However, as Table 2 shows, about 50 percent of tritum is burned, so the maximum N_{nt} < 3, including some initial T load with f=0.1.

Table 3 and Fig. 3 below show predictions of this model for neutron production:

$i =$	Fuel energy $Ef_i =$	Initial T mass $\frac{M_t(2, Ef_i)}{10^{-3}} =$	T-mass bred $\frac{M_{tb}(2, Ef_i)}{10^{-3}} =$	T-mass consumed $\frac{M_{tc}(2, Ef_i)}{10^{-3}} =$	Net T--Mass produnced $\frac{M_{tn}(2, Ef_i)}{10^{-3}} =$	Neutrons per T burned $N_{ndd}(2, Ef_i) =$
1	0.1	0.02	0.01	0.01	-0.0035	1.8
2	0.25	0.07	0.05	0.05	-0.0022	2
3	0.5	0.16	0.14	0.13	0.014	2.2
4	0.85	0.29	0.33	0.27	0.0606	2.3
5	1.3	0.49	0.65	0.49	0.1547	2.4
6	1.85	0.74	1.14	0.82	0.314	2.5
7	2.5	1.05	1.83	1.27	0.5572	2.6
	(MJ)	(mg)	(mg)	(mg)	(mg)	

Note in Table 3 that net tritium self-breeding sufficiency occurs for fuel energies ~> 0.25 MJ for these cases with 1.3 % molar fraction of trutium. We will use this model again later on for α=1.5, so we can better compare with the T-lean examples of Atzeni and Ciampi Nuc. Fusion 37, 1665 (1997) at their closest case with 1 % molar fraction of T. Fig. 3 compares neutrons per T burned and extra available neutrons (neutons produced minus any needed for T breeding) per MeV of fusion yield for the T-lean assembles compared to conventional DT targets, where we assume a typical DT neutron multiplication of 1.4 for FLiBe blankets, but no multiplication for any dd neutrons.

No. of neutrons available (inc. multiplication and minus any needed for T-replacement) per T burned:

For T-lean case $$N_{ndda}(\alpha, E_f) := \left(M_{3Heb}(\alpha, E_f) + 1.4 \cdot M_{tc}(\alpha, E_f)\right) \cdot M_{tc}(\alpha, E_f)^{-1} \quad \text{Eq 18}$$

For DT case $$N_{ndta} := 1.4 - 1 \quad \text{Eq 19}$$

No. of neutrons avaialbe for uses other than T replacement, per MeV of fusion yield

For T-lean case $$NY_{dd}(\alpha, E_f) := N_{ndda}(\alpha, E_f) \cdot \left(\frac{M_d(2, E_f) \cdot 4.6 + M_t(2, E_f) \cdot 17.6}{M_d(2, E_f) + M_t(2, E_f)}\right)^{-1} \quad \text{Eq 20}$$

For DT case $$NY_{dt}(\alpha, E_f) := N_{ndta} \cdot 17.6^{-1} \quad \text{Eq 21}$$

Ratio of neutons available T-lean case over DT case, per MeV yield

$$NpYR(\alpha, E_f) := NY_{dd}(\alpha, E_f) \cdot NY_{dt}(\alpha, E_f)^{-1} \quad \text{Eq 22}$$

Fig 3: Neutrons produced per T burned and the ratio of available neutons per MeV yield vs fuel energy.

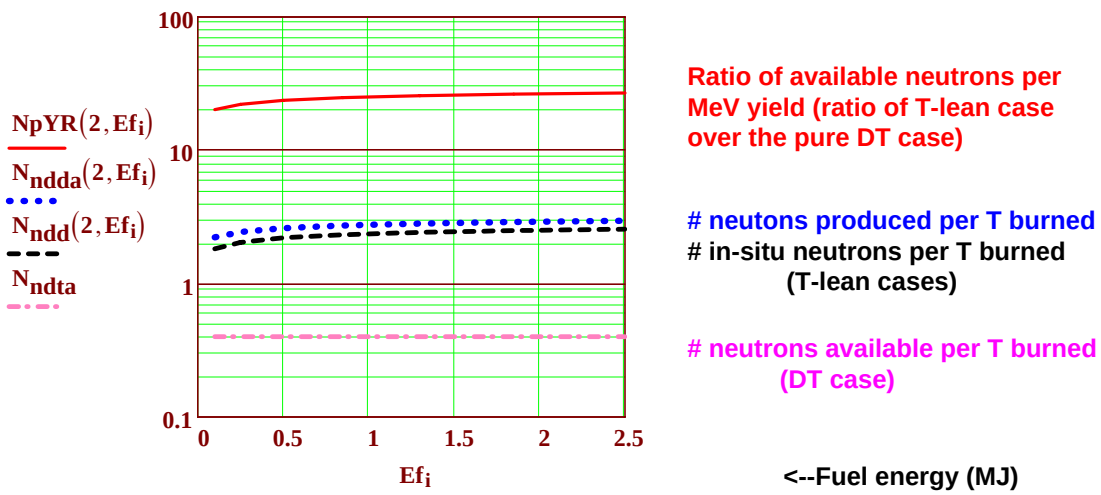

Figure 3 shows that T-lean targets can be 30 times more prolific neutron sources per fusion watt for purposes of various applications in blankets compared to DT targets, besides being tritium self-sufficient (sufficient in-situ breeding so that blanket material options are not restricted to contain lithium).

The copious extra neutrons available with T-lean targets, as pointed out by Tabak[1], can be used in external blankets of different materials, (in some cases without lithium if desired) for several purposes:
(a) generate extra energy for direct conversion through exothermic neutron capture
(b) generate extra tritium for sale to other tritium-deficient reactors like ITER
(c) breed fissile fuel sufficient to support many client fission reactors

Table 4 compares the Tabak-based model @ adiabat α=1.5 with the closest Atzeni/Ciampi's T-lean example for marginal net T-sufficiency at adiabat α=1.5. The Tabak-based model is based on isobaric DT hotspot ignition, while the Atzeni/Ciampi model is based on isochoric fast ignition. We assume the Tabak model would also be consistent with the new Betti-Perkins variant of hot spot ignition with a late shock but without needing a fast igniter pulse (easier for ion beam drive), in case implosions don't quite reach the 10 keV hot spot DT temperatures postulated in the beginning of Max's burn calculations.

Table 4	Atzeni/Ciampi example	Tabak-based MCAD Model
Molar T-fraction	1 %	1.3 %
Adiabat α	1.5	1.5
Fuel energy (MJ)	1	1
Fuel Mass (g)	0.020	$M_d(1.5,1) + M_t(1.5,1) = 0.023$
Fuel density (g/cm^3)	800	$\rho_{cdd}(1.5,1) = 659$
Fuel Rho-r (g/cm^2)	10.7	$\rho r(1.5,1) = 9.9$
Fuel gain G_f *and Fusion Yield* (in MJ)	1050	$G_f(1.5,1) = 494$

Note that despite the difference in the two ignition/burn models, these cases compare reasonably at similar dd fuel masses and fuel energies at comparable seed molar tritium fractions and both at marginal T self-breeding sufficiency. If anything, the Tabak-based model is pessimistic with repect to the Atzeni/Ciampi calculation. We should expect the higher fuel gain for the Atzeni/Ciampi isochoric ignition assumption compared to the isobaric ignition Tabak-based MCAD model. We prefer the latter approach anyway because its easier to drive with mm-spot radius ion beams (no fast ignition requirement), and because ion accelerators are more efficient, so don't require as high a fuel gain. We'll be estimating the ion direct drive implosion requirements and coupling efficiency shortly, where we will find that driving hydrogen ablators with appropriate range ions at the peak rocket efficiency η_r = 65% --> capsule drive efficiencies η_c~ 0.33, so that a 1 MJ fuel assembly energy implies a very reasonable 3 MJ ion beam driver energy, and overall gains $\eta_c G_f$ > 160, much more than needed for accelerator driver efficiencies η_d high enough for $\eta_d \eta_c G_f$ > 10. We'll use the Tabak-based case in Table 4 for a reference case full scale power plant, and then one with a 1 MJ driver for a DEMO.

Direct MHD conversion. Next, lets look at the potential to use these T-lean cases for low-cost Balance-of-Plant with direct plasma MHD conversion, based on the Compact Fusion Advanced Rankine (CFAR) cycle[2] , in which a small vaporizable/ionizable/recylable shell material is inserted around and simultaneously with each target (See Fig. 4 below). The shell has 5% solid angle holes for driver beam access, and is used to capture target charged-particle, x-ray, and at least half of the remaining neutron energy *escaping the target* to create 1 to 2 eV dense chamber plasma for direct conversion. As indicated in ref. 1, most of the neutron energy is internally captured in T-lean cases because the fuel ρr exceeds the neutron mean-free-path. Thus, a thin (1 mm) lead layer lines the inner surface of the target shell to capture the 40 % of T-lean target output in the form of 100 keV x-rays. The bulk of the target shell consists of some hydrogen hydride to efficiently absorb neutron energy (which may also provide some energy multiplication through exothermic neutron capture), and is capped by an outer layer of alkali metal such as Potassium to enhance the plasma conductivity of the subsequent mix for efficient (>50 % direct) MHD conversion.

[2] B. Grant Logan "Inertial fusion reactors using Compact Fusion Advanced Rankine (CFARII) MHD Conversion" Fusion Engineering and Design 22, 151 (1993)

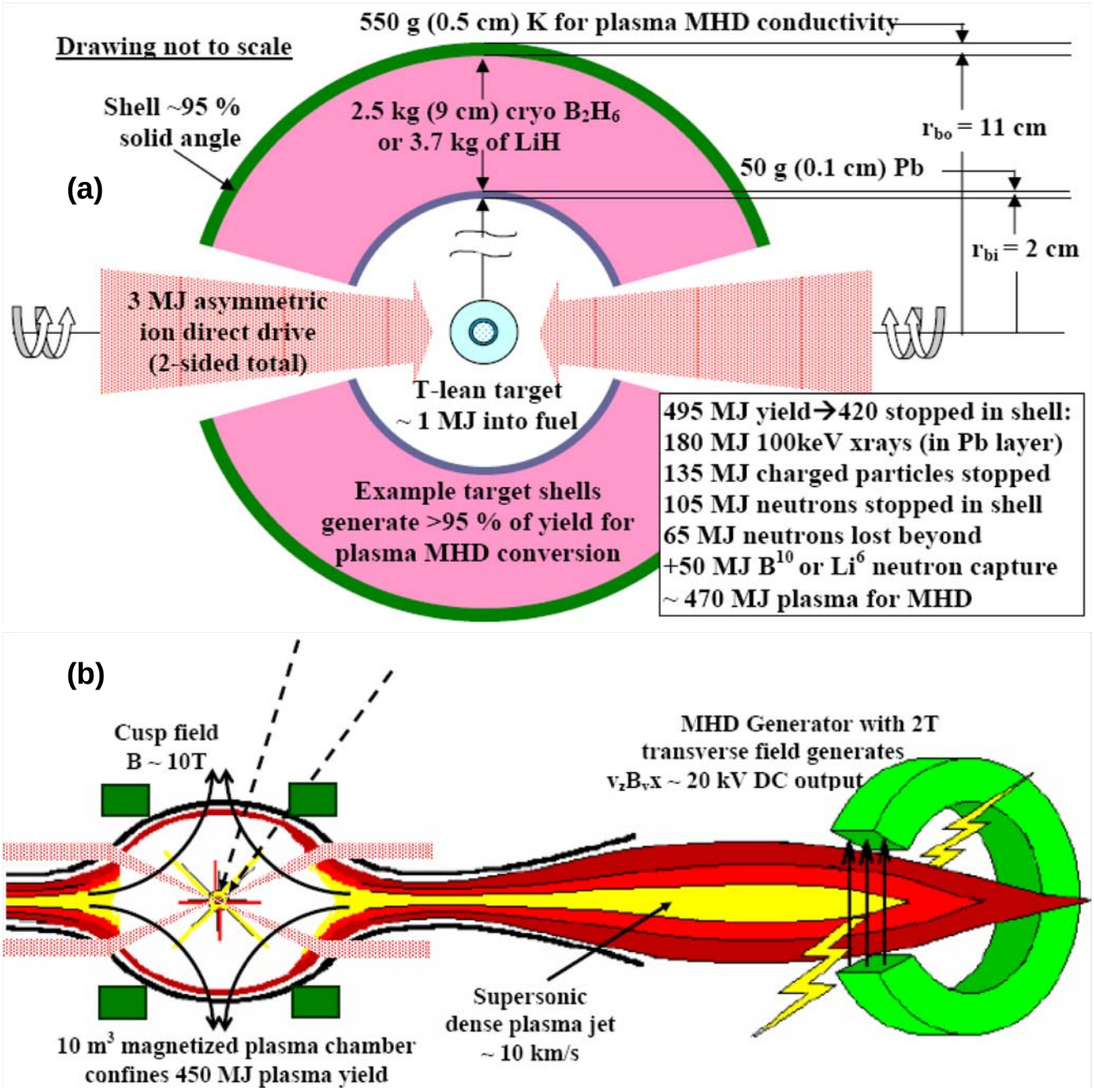

Figure 4: (a) Example target shell for efficient conversion of T-lean target output into 1 to 2 eV dense plasma for direct MHD conversion. All shell materials condense and recycle (Rankine cycle).
(b) Schematic of the CFAR MHD scheme (adapting the old 1992 CFAR Logo!)--no detailed design yet.

Note some key facts about the marriage of T-lean targets to CFAR energy conversion:
(1) A 10 T cusp field on a 2-m vessel/coil radius with a protective 0.6 m-thick Flibe vortex layer inside aids final focusing of ion beams and prevents large shocks to the vessel wall with large yields. The plasma created from the T-lean target shell is conductive enough for the field to confine the 470 MJ plasma until drained out through the MHD generators in ~50 ms. Unlike ref. 2, we assume here < 50 % duty factor for MHD generation to allow the chamber pressure to drop to low values for target insertion. 65 MJ of neutrons + 15 MJ of x-rays <u>not</u> stopped in the target shell act like a small 80 MJ yield in the 10 m^3 Flibe vortex pocket.
(2) Because plasma conductivity is 10^5 times greater at 25,000 K than at 2500 K, the extractable MHD conversion power density ~σu^2, where u~10km/s is the plasma jet velocity, is <u>>30 times the power density of steam turbine generators</u>. As a consequence, the CFAR BoP cost can be much lower, < $ 80 M/ GWe.[2]

Scaling of capture fractions of T-lean target outputs into plasma for direct conversion.

Fraction of yield born in neutrons (neglecting inelastic neutron scattering)

$$FY_{no}(\alpha, E_f) := \frac{14.1 \cdot 17.6^{-1} \cdot 5 \cdot 3^{-1} \cdot M_t(\alpha, E_f) \cdot f_{bt}(\alpha, E_f) \cdot (3.37 \cdot 10^5) \ldots + M_d(\alpha, E_f) \cdot f_{bd}(\alpha, E_f) \cdot \left[2.45 \cdot 7.31^{-1} \cdot 8.85 \cdot 10^4 \ldots + 0.625 \cdot f_{bt}(\alpha, E_f) \cdot (14.1 \cdot 17.6^{-1}) \cdot 3.37 \cdot 10^5 \right]}{Y_f(\alpha, E_f)} \quad \text{Eg 23}$$

Fig. 5 Neutron energy loss in hydrogen

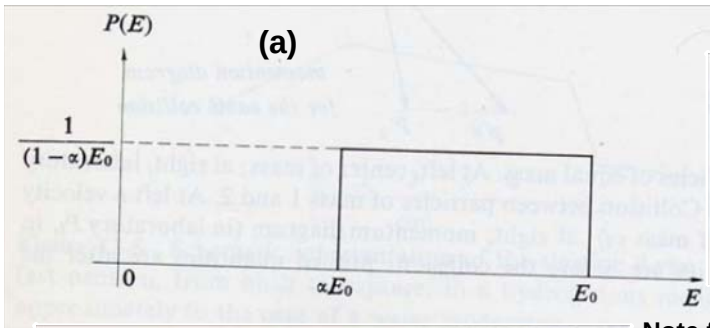

Distribution of the values of the neutron energy E after one collision in the case of isotropic scattering in the center-of-mass system for a neutron of initial energy E_0. The quantity $\alpha = (A-1)^2/(A+1)^2$.

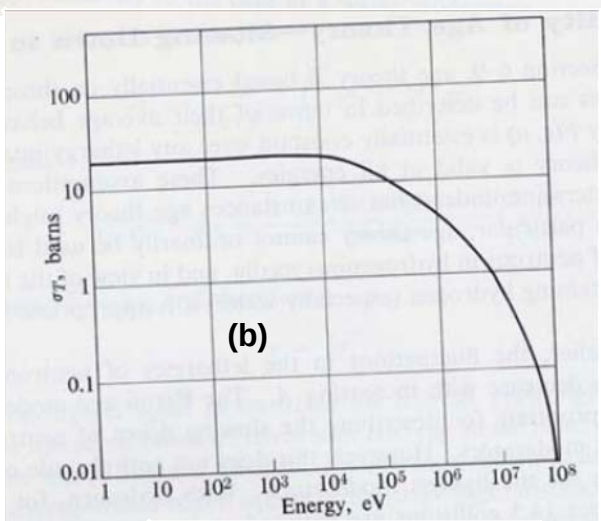

The total cross section of hydrogen.

Note for hydrogen in the target shell, this $\alpha = 0$, for deuterium in the target, $\alpha = 0.11$. For hydrogen/deuterium, neutrons don't diffuse much further from the point they have their first inelastic collision. For 14 MeV neutrons from DT, the efolding ρr in hydrogen is 5 g/cm^2, or 10 g/cm^2 in deuterium, neglecting the neutron's cross section contribution in the deuterium nucleus. For 2.5 MeV neutrons from DD, the e-folding ρr is about 0.7 g/cm^2 in H, or 1.4 g/cm^2 in D. As we will see, the T-lean targets reduce the escaping neutron energy ~50% as in this Fig 5(a), going into the shell.

--->Estimated neutron e-folding ρr's:

$\rho r_{14D} := 10$	$\rho r_{14H} := 5$	$\rho r_{7H} := 2$
$\rho r_{2.5D} := 1.4$	$\rho r_{2.5H} := 0.7$	$\rho r_{1.2H} := 0.4$
in the target	all g/cm^2	in the shell

Neutron energy attenuation factors A.

The average ρr a neutron has to go to escape in the target depends on where it is born, so we need to define some spatial weigting factors fs when using the total target fuel ρr :

$fsdti := 1$	$A_{nt}(\alpha, E_f) := \exp\left(-fsdti \cdot \rho r(\alpha, E_f) \cdot \rho r_{14D}^{-1}\right)$	for DT neutrons from hot spot	Eq 24
$fsddo := 0.2$	$A_{nd}(\alpha, E_f) := \exp\left(-fsddo \cdot \rho r(\alpha, E_f) \cdot \rho r_{2.5D}^{-1}\right)$	outer-born DD neutrons	Eq 25
$fsdto := 0.4$	$A_{ndt}(\alpha, E_f) := \exp\left(-fsdto \cdot \rho r(\alpha, E_f) \cdot \rho r_{14D}^{-1}\right)$	outer-born DT neutrons	Eq 26

The weighting factor for 2.5 MeV deuterons should be less than the dd-mass weighting 0.33, while the outer-born DT neutrons should be a bit more than 0.33, because the burn wave T increases with r.

Model fraction of fusion energy escaping as neutrons

$$FY_n(\alpha, E_f) := \frac{14.1 \cdot 17.6^{-1} \cdot 5 \cdot 3^{-1} \cdot M_t(\alpha, E_f) \cdot f_{bt}(\alpha, E_f) \cdot (3.37 \cdot 10^5) \cdot A_{nt}(\alpha, E_f) \ldots + M_d(\alpha, E_f) \cdot f_{bd}(\alpha, E_f) \cdot \left[2.45 \cdot 7.31^{-1} \cdot 8.85 \cdot 10^4 \cdot A_{nd}(\alpha, E_f) \ldots + 0.625 \cdot f_{bt}(\alpha, E_f) \cdot (14.1 \cdot 17.6^{-1}) \cdot 3.37 \cdot 10^5 \cdot A_{ndt}(\alpha, E_f) \right]}{Y_f(\alpha, E_f)} \qquad \text{Eq 27}$$

MTabak results for escaping neutron fraction of yield for his Case C: $FYmt_1 := 0.45$ $FYmt_2 := 0.4$

$FYmt_3 := 0.35$ $FYmt_4 := 0.33$ $FYmt_5 := 0.31$ $FYmt_6 := 0.30$ $FYmt_7 := 0.29$

Now lets add the additional neutron capture in the target shell. To maintain the optimum shell-produced plasma temperature of 1.5 eV for MHD, we need to scale the shell-blanket mass (see figure 4) proportional to captured fusion yield to keep the average enegy deposition in the shell 110 MJ/kg. To simply the estimate, we note that the captured fusion yield is close enough to the fusion yield that we can scale the outer shell-blanket radius r_{bo} simply as:

$$r_{bo}(\alpha, E_f) := 11 \cdot \left(Y_f(\alpha, E_f) \cdot Y_f(2, 1)^{-1} \right)^{0.333} \quad \text{(cm)} \qquad \text{Eq 28}$$

The resulting additional attenuation (capture) of neutron energy for direct conversion purposes (fraction of yield finally escaping both the target and the shell), estimating attenuation by hydrogen component density in the shell, and augmenting that by 25% to account for Boron/Lithium capture.

$\rho_{Hb} := 0.12$ g/cm^3 density of hydrogen in balnket shell

$$A_{ntb}(\alpha, E_f) := \exp\left[-1.25 \cdot \rho_{Hb} \cdot (r_{bo}(\alpha, E_f) - 2) \cdot \rho r_{7H}^{-1} \right] \qquad \text{Eq 29}$$

$$A_{ndb}(\alpha, E_f) := \exp\left[-1.25 \cdot \rho_{Hb} \cdot (r_{bo}(\alpha, E_f) - 2) \cdot \rho r_{1.2H}^{-1} \right] \qquad \text{Eq 30}$$

$$FY_{nb}(\alpha, E_f) := \frac{14.1 \cdot 17.6^{-1} \cdot 5 \cdot 3^{-1} \cdot M_t(\alpha, E_f) \cdot f_{bt}(\alpha, E_f) \cdot (3.37 \cdot 10^5) \cdot A_{nt}(\alpha, E_f) \cdot A_{ntb}(\alpha, E_f) \ldots + M_d(\alpha, E_f) \cdot f_{bd}(\alpha, E_f) \cdot \left[2.45 \cdot 7.31^{-1} \cdot 8.85 \cdot 10^4 \cdot A_{nd}(\alpha, E_f) \cdot A_{ndb}(\alpha, E_f) \ldots + 0.625 \cdot f_{bt}(\alpha, E_f) \cdot \left(\frac{14.1}{17.6}\right) \cdot 3.37 \cdot 10^5 \cdot A_{ndt}(\alpha, E_f) \cdot A_{ntb}(\alpha, E_f) \right]}{Y_f(\alpha, E_f)} \qquad \text{Eq 31}$$

Table 5 blanket radius & loss -yield ration vs fuel energy

$Ef_i =$	$\rho r(2, Ef_i) :$	$Y_f(2, Ef_i) :$	$r_{bo}(2, Ef_i)$	$FY_{nb}(2, Ef_i) =$
0.1	5.4	11	3.6	0.37
0.25	6.4	40	5.6	0.28
0.5	7.3	111	7.8	0.21
0.85	8.1	245	10.1	0.17
1.3	8.8	466	12.6	0.13
1.85	9.4	798	15	0.1
2.5	10	1268	17.5	0.08
MJ	g/cm^2	MJ	cm	

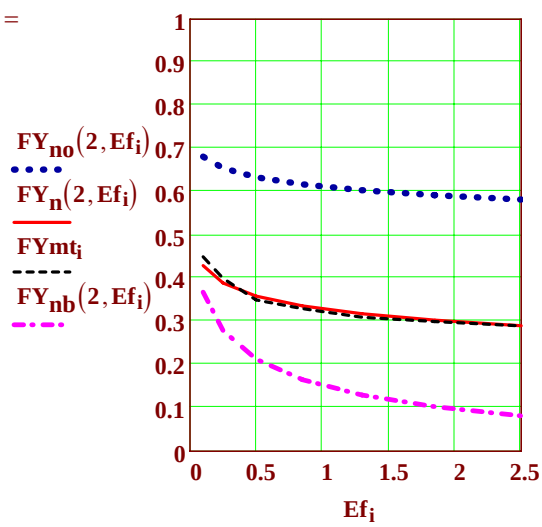

Figure 6. Fraction of total T-lean target yield escaping target and shell as neutrons as a function of fuel energy E_f (adiabat α=2). The model (solid red curve), and Max Tabak's case C runs agree well and show signficant reduction of lost neutron energy below the un-attenuated neutron yield (blue dotted line) within the large ρr of T-lean targets. The shell captures ~ 50% of remaining neutron energy escaping the target (depending on the fuel ρr- see dashed magenta curve for FY_{nb}).

Rocket efficiency and implosion efficiency with pure H2 ablators. We assume a pure hydrogen ablator for ion beam direct drive because hydrogen provides the highest exhaust velocity for ablative drive for a given specific energy deposition by short range ions. Working backwards, we will estimate specific ion beam requirements at the end. We assume thin coatings between the DT, DD, and H ablator layers such that the hot spot decay heat gives equilbrium temperatures of 19-->14-->10 deg K for these layers respectively. The DT layer would be filled through the hydrogen layer by a thin fill tube.

Figure 7: the classic spherical rocket efficiency η_r as a function of the fractional payload mass

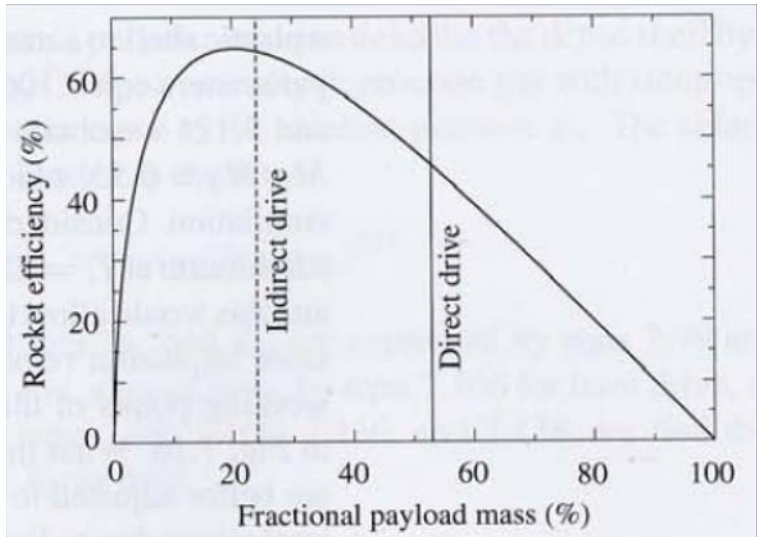

An issue is managing space charge in accelerators delivering the energy with short enough range ions to avoid too much ablation. Another factor can be ionization energy losses which reduce the capsule hydro efficiency η_c below the rocket efficiency η_c. However, since pure hydrogen has a small ionization energy of 13.6 eV per atom, we don't worry about the latter so much. So, from Fig. 7, we choose to drive at the peak rocket efficiency

$\eta_r := 0.65$

with an associated fractional payload mass $M_1 = 0.2\ M_0$, which requires an H_2 ablator mass M_h:

$$M_h(\alpha, E_f) := 4\cdot\left(M_d(\alpha, E_f) + M_t(\alpha, E_f)\right) \quad \text{(g).} \qquad \text{Eq 32}$$

The implosion velocity u_{imp} is that required to create the fuel internal energy E_f upon stagnation:

$$u_{imp}(\alpha, E_f) := \left[2\cdot E_f\cdot 10^{13}\cdot\left(M_d(\alpha, E_f) + M_t(\alpha, E_f)\right)^{-1}\right]^{0.5} \quad \text{(cm/s).} \qquad \text{Eq 33}$$

The ablation exhaust velocity u_{ex} for the chosen peak rocket efficiency is given by

$$u_{ex}(\alpha, E_f) := u_{imp}(\alpha, E_f)\cdot \ln(5)^{-1} \quad \text{(cm/s)} \qquad \text{Eq 34}$$

Figure 8. Shell radius versus fractional exhaust mass for various implosion parameters

$\varepsilon = \varepsilon_{imp} = m_{adot}\ R_0/(u_{ex}\rho_0\Delta R_0)$ Eq. 35

For the chosen fractional exhaust mass = 80%, Fig. 8 indicates a minimum implosion parameter:

$\varepsilon_{imp} := 1.6 \qquad \ln(5) = 1.6$

$\rho_{Ho} := 0.1$ g/cm^3 for H_2 ablator ρ_0

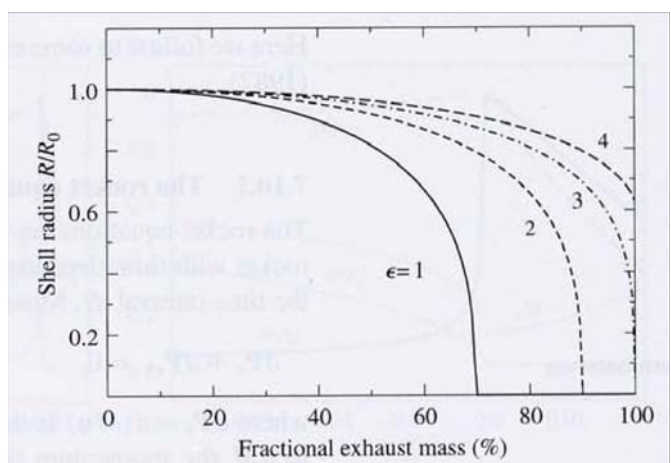

For good hydrodynamic stability during implosion, we choose a moderate in-flight aspect ratio $A_{if} = \rho_a R_0 / (\rho_0 \Delta R_0)$: (half the "usual" value 30), where ρ_a is the density of the compressed in-flight shell. Typically, $\rho_a \sim 5\,\rho_0$, so the initial aspect ratio $A_{in} = R_0/\Delta R_0 \sim 3$. This initial aspect ratio and the known iniital densities and masses of hydrogen and deuterium allows us to find the outer radius r_a of the hydrogen ablator (we neglect the 1 % DT hotspot mass in this calculation). The initial deuterium layer thickness δD and the outer hydrogen ablator radius r_a are solved:

$A_{if} := 15$ Eq. 36

$\rho_a := 5 \cdot \rho_{Ho}$ Eq. 37

$A_{in} := 3$ $\xi := 1 - A_{in}^{-1}$

$\rho_{Do} := 0.2$ g/cm^3 for D_2 intial ρ_0

$m_h := 1.67 \cdot 10^{-24}$ g/H atom

Given Initial guesses $r_{ag} := 0.5$ cm $\delta D := 0.1$ cm

$$\delta D = \left[\left(\frac{3 \cdot M_d(\alpha, E_f)}{4 \cdot \pi \cdot \rho_{Do}}\right) + (\xi \cdot r_{ag})^3\right]^{0.333} - \xi \cdot r_{ag}$$

$$r_{ag} = \left[\left(\frac{3 \cdot M_h(\alpha, E_f)}{4 \cdot \pi \cdot \rho_{Ho}}\right) + (\xi \cdot r_{ag} + \delta D)^3\right]^{0.333}$$

$Sol(\alpha, E_f) := Find(\delta D, r_{ag})$

$\delta_D(\alpha, E_f) := Sol(\alpha, E_f)_1$ Initial D2 layer thickness Eq 38

$r_a(\alpha, E_f) := Sol(\alpha, E_f)_2$ Initial outer H2 ablator radius Eq 39

The total required driver energy E_d input is higher than the radial KE~0.5 $M_h\, u_{ex}^2$ because of
(1) hydrogen ionization energy of 13.6 eV/atom x 2 to account for associated radiation loss,
(2) $3T_{ex}$ temperature-gas energy carried by exhaust plasma implied by $u_{ex} = 2c_T = 2[2\gamma T/m_h]^{0.5}$ Eq 40
(3) energy E_s required to pre-compress the D+DT payload to the in-flight shell density ρ_a:

Shell compression $E_{cs}(\alpha, E_f) := 0.67 \cdot \alpha \cdot \rho_a^{0.67} \cdot (M_h(\alpha, E_f) + M_d(\alpha, E_f) + M_t(\alpha, E_f))$ (MJ) Eq 41

Exhaust temp. $T_{ex}(\alpha, E_f) := 3 \cdot 10^{-4} \cdot m_h \cdot u_{ex}(\alpha, E_f)^2 \cdot 200^{-2} \cdot (1.6 \cdot 10^{-19})^{-1}$ (eV) Eq. 42

One can check that the hydrogen ablator is optically thick at the temperature T_{ex}, but the black body radiation loss is negligible because T_{ex} is so low. The resulting total driver energy required is then:

$$E_d(\alpha, E_f) := 0.5 \cdot 10^{-13} \cdot M_h(\alpha, E_f) \cdot u_{ex}(\alpha, E_f)^2 \ldots + (13.6 \cdot 2 + 3 \cdot T_{ex}(\alpha, E_f)) \cdot 1.6 \cdot 10^{-25} \cdot M_h(\alpha, E_f) \cdot m_h^{-1} \ldots + E_{cs}(\alpha, E_f)$$ (MJ) Eq. 43

The ion direct drive capsule implosion efficiency and target gain vs fuel energy. Results are summarized in Table 6.

$\eta_c(\alpha, E_f) := E_f \cdot E_d(\alpha, E_f)^{-1}$ Eq. 44

$G_t(\alpha, E_f) := \eta_c(\alpha, E_f) \cdot G_f(\alpha, E_f)$

Table 6: T-lean implosion efficiency and gain vs fuel energy.

$Ef_i =$	$E_d(1.5, Ef_i)$	$\eta_c(1.5, Ef_i) =$	$G_t(1.5, Ef_i) =$	$u_{imp}(1.5, Ef_i)$	$u_{ex}(1.5, Ef_i) =$	$T_{ex}(1.5, Ef_i)$	$r_a(1.5, Ef_i) =$	
0.1	0.24	0.41	65	$3.7 \cdot 10^7$	$2.3 \cdot 10^7$	41	0.28	
0.25	0.62	0.404	98	$3.4 \cdot 10^7$	$2.1 \cdot 10^7$	35	0.41	
0.5	1.26	0.398	136	$3.2 \cdot 10^7$	$2 \cdot 10^7$	30	0.54	<--DEMO
0.85	2.16	0.393	178	$3 \cdot 10^7$	$1.9 \cdot 10^7$	27	0.66	
1.3	3.34	0.389	222	$2.9 \cdot 10^7$	$1.8 \cdot 10^7$	25	0.78	<--Power Plant
1.85	4.79	0.386	267	$2.8 \cdot 10^7$	$1.7 \cdot 10^7$	23	0.9	
2.5	6.53	0.383	314	$2.7 \cdot 10^7$	$1.7 \cdot 10^7$	22	1.02	
MJ	MJ			cm/s	cm/s	eV	cm!	